

Superconductivity in TlBi₂ with a large Kadowaki-Woods ratio

Zihua Yang,¹ Zhen Yang,¹ Qiping Su,¹ Jianhua Du,² Enda Fang,¹ Chunxiang Wu,³ Jinhu Yang,¹ Bin Chen,¹ Hangdong Wang,^{1,*} and Minghu Fang^{3,4,†}

¹Hangzhou Key Laboratory of Quantum Matter, School of Physics, Hangzhou Normal University, Hangzhou 311121, China

²Department of Physics, China Jiliang University, Hangzhou 310018, China

³Department of Physics, Zhejiang University, Hangzhou 310027, China

⁴Collaborative Innovation Center of Advanced Microstructures, Nanjing University, Nanjing 210093, China

(Dated: April 12, 2022)

In this article, the superconducting and normal state properties of TlBi₂ with the AlB₂-type structure were studied by the resistivity, magnetization and specific heat measurements. It was found that bulk superconductivity with $T_C = 6.2$ K emerges in TlBi₂, which is a phonon-mediated s -wave superconductor with a strong electron-phonon coupling ($\lambda_{ep} = 1.38$) and a large superconducting gap ($\Delta_0/k_B T_C = 2.25$). We found that the $\rho(T)$ exhibits an unusual T -linear dependence above 50 K, and can be well described by the Fermi-liquid theory below 20 K. Interestingly, its Kadowaki-Woods ratio A/γ^2 [$9.2 \times 10^{-5} \mu\Omega \text{ cm}(\text{mol K}^2/\text{mJ})^2$] is unexpectedly one order of magnitude larger than that obtained in many heavy Fermi compounds, although the electron correlation is not so strong.

I. INTRODUCTION

MgB₂, as a simple binary compound, has a rather high superconducting transition temperature ($T_C = 39$ K) compared with other conventional superconductors^{1,2}. The first-principles calculations and the inelastic neutron scattering measurements revealed that the E_{2g} in-plane boron phonons near the Brillouin zone center strongly coupled to the planar boron σ bands^{3,4}, which leads to the high T_C in MgB₂. Moreover, MgB₂ has the multiple bands with a weak electron correlation⁵⁻⁷, and the distinct multiple superconducting energy gaps^{8,9}, resulting in markedly novel behaviors in its superconducting and normal-state properties². Although MgB₂ has been extensively studied, new physical phenomena are constantly discovered^{10,11}, so those superconductors with the same structure are worth revisiting.

The binary bismuthide TlBi₂¹² crystallizes in a hexagonal AlB₂-type structure as the same as MgB₂, consisting of honeycombed bismuth layers and thallium layers located in between them, as shown in the inset of Fig. 1. Compared with MgB₂, TlBi₂ contains the heavier elements, suppressing the high frequency lattice vibration, and being unfavorable to the high T_C superconductivity in the conventional electron-phonon coupling mechanism. Although TlBi₂ was classified into a strong coupling superconductor with $T_C = 6.4$ K by R. Dynes in 1972¹³, its detailed physical properties are rarely investigated as comparison with MgB₂.

In this article, we synthesized successfully the single phase polycrystalline TlBi₂ sample. The superconducting and normal state properties were systematically studied by resistivity, magnetization, Hall resistivity and specific heat measurements. We reconfirmed that type-II superconductivity with $T_C = 6.2$ K, the upper critical field $\mu_0 H_{c2} = 1.4$ T, and the lower critical field $\mu_0 H_{c1} = 1.08 \times 10^{-2}$ T emerge in TlBi₂ compound. It was found that the electronic specific heat in the supercon-

ducting state can be well described using a single gap model within Bardeen-Cooper-Schrieffer (BCS) framework. The strong electron-phonon coupling occurs in this compound, confirmed by both the large λ_{ep} ($= 1.38$) and the large $\Delta_0/k_B T_C$ ($= 2.25$) values, indicating that TlBi₂ is a conventional superconductor. It was found that the temperature dependence of resistivity in the normal state, $\rho(T)$, exhibits an unusual linear behavior above 50 K, which is ascribed to the low-energy phonon scattering, while $\rho(T)$ below 20 K is well described by the Fermi liquid theory, *i.e.*, $\rho(T) = \rho_0 + AT^2$. Combining the specific heat data at normal state, we found that its Kadowaki-Woods ratio (KWR), A/γ^2 [$9.2 \times 10^{-5} \mu\Omega \text{ cm}(\text{mol K}^2/\text{mJ})^2$], is unexpectedly one order of magnitude larger than that obtained in many heavy Fermi compounds, although the electron correlation is not so strong.

II. EXPERIMENTAL METHODS

TlBi₂ polycrystalline samples were synthesized using the method as described before¹⁴. First, Tl and Bi lumps were mixed and sealed in a vacuum quartz tube. Then, the mixture was molten over a flame and mixed carefully by shaking vigorously for 10 min. After that, TlBi₂ samples were annealed at 210 °C for 2 weeks. At last, the quartz tube was quenched into cold water to prevent the formation of impurity phases during cooling process. In order to compensate for the loss of Tl due to the presence of Tl₂O₃ in the raw material, an additional 10% Tl was added. The obtained sample was easy to press into a flake and then cut into rectangular bars for later study. Polycrystalline x -ray diffraction (XRD) was performed on a Rigaku x -ray diffractometer with Cu K_α radiation. The resistivity and Hall coefficient were measured using the standard four-probe technique. The heat capacity was measured using the relaxation method. All the transport

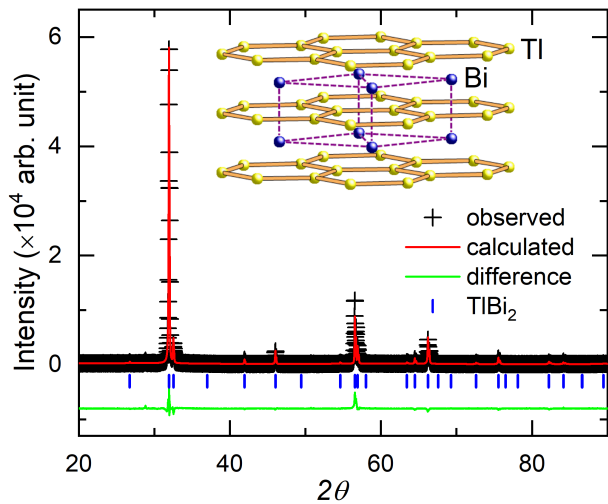


FIG. 1. (Color online) Rietveld refinement profile of the polycrystalline XRD of TlBi_2 . Inset: The crystal structure of TlBi_2 . Thallium and bismuth atoms are drawn as dark blue and yellow spheres, respectively.

properties were measured in a *QuantumDesign* Physical Properties Measurement System PPMS-9. The dc magnetization was obtained using a Magnetic Property Measurement System (*Quantum Design* MPMS-VSM).

III. RESULTS AND DISCUSSIONS

Figure 1 shows the XRD pattern of TlBi_2 sample. All the peaks can be well indexed with an AlB_2 -type structure (space group: $P6/mmm$, *No.* 191), and no obvious impurity peaks were observed. The lattice parameters $a = 5.68(2)$ Å, and $c = 3.37(1)$ Å, were obtained by Rietveld refinement, which is consistent with the results reported previously¹². The cell parameter a of TlBi_2 is much larger than that of MgB_2 and c is smaller, which originates from the nearly same Bi-Bi bond length along the a and c axis, implying its three-dimensional feature.

Figure 2(a) displays the temperature dependence of the resistivity, $\rho(T)$, between 2 and 300 K of TlBi_2 sample. The room temperature resistivity $\rho(300\text{K})$ is about $103.7 \mu\Omega \text{ cm}$, close to that of TlSb ¹⁵. It's clear that TlBi_2 exhibits a metallic behavior in the whole measuring temperature range, *i.e.*, the resistivity decreases with decreasing temperature. At $T_C^{\text{onset}} = 6.25$ K, the resistivity drops abruptly to zero, suggesting that a bulk superconducting transition occurs with a transition width $\Delta T_C = 0.05$ K, which is also confirmed by a large diamagnetic signal and a significant specific heat jump at T_C , as shown in Fig. 2(c) and Fig. 3, respectively. The superconducting transition temperature here is similar to that reported previously ($T_C = 6.4$ K)¹³.

It is obvious that the $\rho(T)$ in the normal state exhibits a linear temperature dependence in a large region ($50 \text{ K} \leq T \leq 300 \text{ K}$), which can be ascribed to the low-energy

phonon scattering here¹⁶, although the similar behavior in the cuprate high temperature superconductors was explained as the strong electron correlation effect. As shown by a blue line in the Fig. 2(a), we fitted the $\rho(T)$ data above 50 K using the standard Bloch-Grüneisen (BG) formula,

$$\rho = \rho_0 + 4C \left(\frac{T}{\Theta_D} \right)^5 \int_0^{T/\Theta_D} \frac{x^5}{(e^x - 1)(1 - e^{-x})} dx \quad (1)$$

then we obtained the residual resistivity $\rho_0 = 41 \mu\Omega \text{ cm}$, the fitting parameter $C = 17.5 \mu\Omega \text{ cm/K}$, and the Debye temperature $\Theta_D = 83$ K. We also found that the $\rho(T)$ below 50 K deviates from the T -linear dependence and turns to T -square dependence below 20 K, indicating the Fermi-liquid ground state, discussed in details as follows.

In order to obtain the upper critical field $H_{c2}(T)$, we measured the resistivity at various magnetic fields between 2 K and 8 K, as shown in Fig. 2(b). With increasing magnetic field, the superconducting transition shifts to lower temperature. At 2.0 T, the superconducting transition is not observed above 2 K. The H_{c2} is determined by the temperature when the resistivity drops to 50% of the normal state value and is plotted as a function of temperature in the inset of Fig. 2(b). According to the Ginzburg-Landau (GL) theory, the $\mu_0 H_{c2}$ value at zero temperature was estimated to be 1.4 T using the formula

$$H_{c2}(T) = H_{c2}(0)(1 - t^2)/(1 + t^2) \quad (2)$$

where t is the reduced temperature T/T_C . Then the coherence length ξ_{GL} of TlBi_2 was estimated to be 15.3 nm from the relation, $\xi_{GL}^2 = \Phi_0/2\pi H_{c2}(0)$, where $\Phi_0 = h/2e$ is the magnetic flux quantum ($\approx 2.07 \times 10^{-15}$ Wb).

Figure 2(c) shows the temperature dependence of the magnetic susceptibility, $\chi(T)$, measured at an applied field of 5 Oe both in the zero field cooling (ZFC) and field-cooling (FC) processes. A sharp superconducting transition and a quite flat feature below T_C are clearly observed in $\chi(T)$, suggesting superconductivity emerges in the sample. At $T = 2$ K, the $4\pi\chi$ value exceeds -100% eum/cm³ due to the demagnetization effect. The $M(H)$ curve measured at $T = 2$ K, as shown in the inset of Fig. 2(c), exhibits a typical type-II superconducting behavior.

To obtain the lower critical field $H_{c1}(T)$, we measured the $M(H)$ curves at different temperatures, as shown in Fig. 2(d). The $H_{c1}(T)$ determined by the field where M starts to deviate from the initial linear curve, is plotted as a function of temperature in the inset of Fig. 2(d). It is clear that the H_{c1} can be well described using the GL theory as

$$H_{c1}(T) = H_{c1}(0) \left[1 - \left(\frac{T}{T_C} \right)^2 \right] \quad (3)$$

The lower critical field at zero temperature, $H_{c1}(0)$, was estimated to be 108 Oe. The penetration depth λ_{GL} was estimated to be 198 nm using the relation $H_{c1}(0) =$

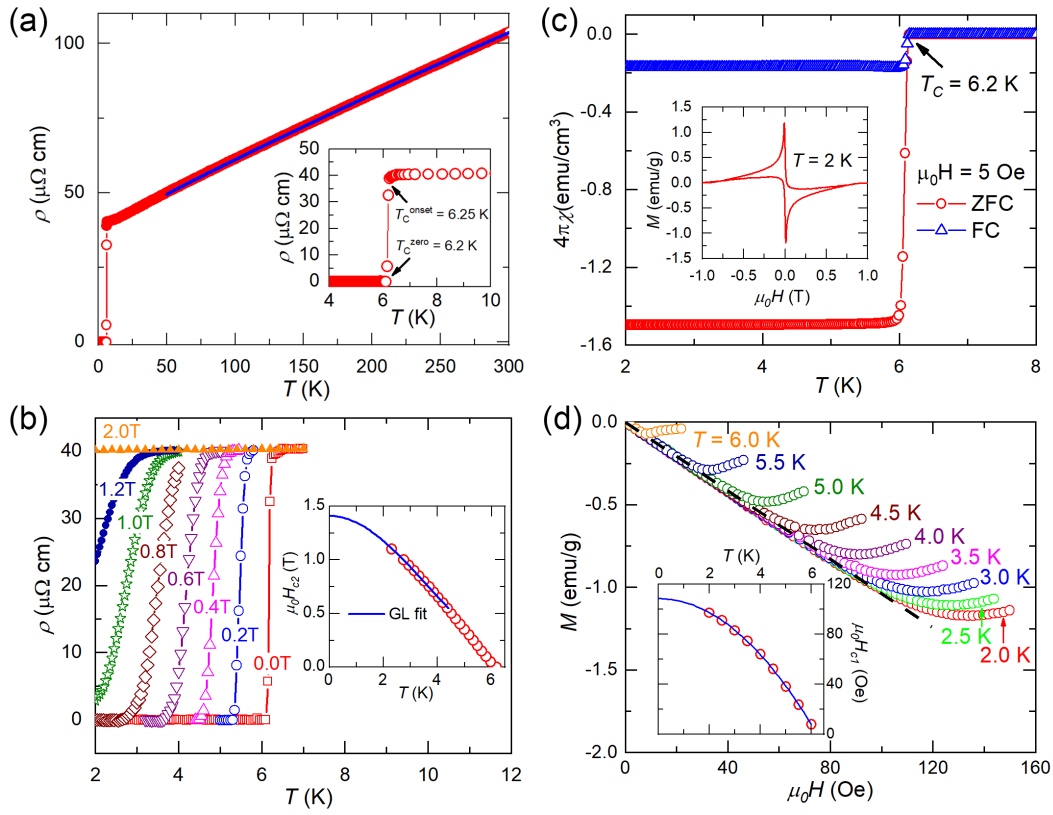


FIG. 2. (color online) (a) Temperature dependence of resistivity of TlBi₂ between 2 and 300 K measured at zero field; Inset: The enlarge view near T_C ; (b) Temperature dependence of resistivity under several selected magnetic fields below 8 K; Inset: The upper critical field H_{c2} as a function of temperature for TlBi₂; (c) Temperature dependence of magnetic susceptibility below 8 K, measured at 5 Oe with both ZFC and FC processes; Inset: Field dependent magnetization M measured between -1 and 1 T at 2 K; (d) Field dependent magnetization M measured at various temperatures below 150 Oe. The dashed line indicates the initial linear magnetization curve. Inset: The lower critical field H_{c1} as a function of temperature for TlBi₂.

$\frac{\Phi_0}{4\pi\lambda_{GL}^2} \ln(\frac{\lambda_{GL}}{\xi_{GL}})$ and the ξ_{GL} value obtained above. Then, the GL parameter, $\kappa_{GL} = \lambda_{GL}/\xi_{GL}$, was calculated to be 12.9, much larger than $1/\sqrt{2}$, confirming that TlBi₂ is a type-II superconductor. The thermodynamic critical field $H_c(0)$ was also estimated to be 770 Oe from the relation, $H_{c1}(0)H_{c2}(0) = H_c^2(0)\ln\kappa_{GL}$, which is almost an order of magnitude smaller than that of MgB₂².

To get the information of superconducting transition, we also carried out the specific heat, $C(T)$, measurements at both 0 T and 2 T. The inset of Fig. 3 shows the temperature square dependence of C/T with a small difference between the two curves below T_C . The low temperature $C(T)$ measured at 2 T, where bulk superconductivity is completely suppressed, can be well fitted using the Debye model, $C/T = \gamma + \beta T^2 + \delta T^4$, where γ is the Sommerfeld coefficient, β Debye constant, and δ the fitting parameter. The first and last two terms are ascribed to the electronic and phonon contribution, respectively. We obtained $\gamma = 8.63$ mJ/(mol K²), $\beta = 4.87$ mJ/(mol K⁴), and $\delta = 0.35$ mJ/(mol K⁶) by the best fit to the data below 4 K (the solid green line). Then, the Debye temperature Θ_D , was evaluated to be 104 K, which is close to that (83 K) obtained from the $\rho(T)$ data mentioned

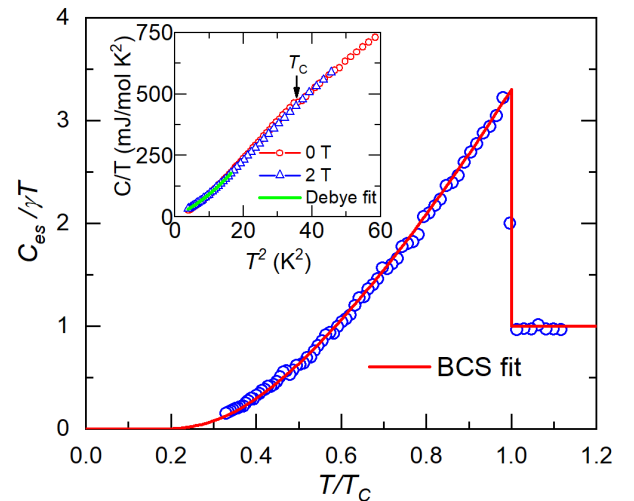


FIG. 3. (Color online) The electronic specific heat divided by the product of Sommerfeld coefficient γ and temperature as a function of the reduced temperature T/T_C in the superconducting state at zero field; Inset: temperature square dependence of C/T , measured at 0 T and 2 T magnetic fields. The green line is the fit to the data as described in the text.

above, from the relation $\Theta_D = (12\pi^4 RN/5\beta)^{1/3}$, where $R = 8.31 \text{ J/(mol K)}$ is the molar gas constant, and N is the number of atoms per unit cell. The electronic specific heat, $C_{es}(T)$, in the superconducting state was obtained by subtracting the phonon contribution from the total $C(T)$. Figure 3 presents the $C_{es}/\gamma T$ vs. T/T_C , a sharp jump of 2.32 emerging at T_C , which is significantly larger than that of the well known BCS theory (1.43), suggesting that the strong electron-phonon coupling occurs in TlBi₂. The electron-phonon coupling constant, λ_{ep} , can be derived from the modified McMillan formula¹⁷⁻¹⁹

$$\lambda_{ep} = \frac{1.04 + \mu^* \ln(\frac{\omega_{ln}}{1.2T_C})}{(1 - 0.62\mu^*) \ln(\frac{\omega_{ln}}{1.2T_C}) - 1.04} \quad (4)$$

where μ^* is the Coulomb pseudopotential, which has been reported to be 0.121¹³, and ω_{ln} is the logarithmic averaged phonon frequency, which can be estimated from the specific heat jump at T_C using the formula¹⁷⁻¹⁹

$$\frac{\Delta C}{\gamma T_C} = 1.43 \times [1 + 53(\frac{T_C}{\omega_{ln}})^2 \ln(\frac{\omega_{ln}}{3T_C})] \quad (5)$$

Taking $\Delta C/\gamma T_C = 2.32$ and $T_C = 6.2 \text{ K}$, we obtained $\omega_{ln} = 63.3 \text{ K}$ and $\lambda_{ep} = 1.38$, which is smaller than $\lambda_{ep} = 1.63$ reported previously¹³. However, it is still large compared with those for typical strong coupling superconductors such as Mo₆Se₈ ($\lambda_{ep} = 1.27$), and Pb-Tl alloy ($\lambda_{ep} = 1.15$ - 1.53)¹⁷, indicating the strong-coupling nature of superconducting pairing.

Then, we analysed the electronic specific heat data $C_{es}(T)$ using BCS theory with a single gap. Within the framework of BCS theory, the thermodynamic properties, entropy (S) and electronic specific heat (C_{es}), can be written as

$$S = -\frac{6\gamma}{\pi^2} \frac{\Delta_0}{k_B} \int_0^\infty [f \ln f + (1-f) \ln(1-f)] dy \quad (6)$$

$$C_{es} = T \frac{dS}{dT} \quad (7)$$

where $f = [\exp(\beta E) + 1]^{-1}$ and $\beta = (k_B T)^{-1}$, whereas the integration variable is $y = \varepsilon/\Delta_0$. The energy of the quasiparticles is evaluated from the relation $E = [\varepsilon^2 + \Delta_0^2 \delta^2(t)]^{0.5}$, where ε is electron energy with respect to the Fermi energy and $\delta(t)$ is the normalized BCS gap at the reduced temperature $t = T/T_C$ as tabulated by Mühlshlegel²⁰. As shown in the figure, the single-gap model presents a good fit to $C_{es}/\gamma T$, suggesting that TlBi₂ is a phonon-mediated s -wave superconductor. Meanwhile, the $\Delta_0/k_B T_C$ was fitted to be 2.25, agrees well with that obtained from the tunneling experiments²¹, which is much larger than that as predicted for a weak coupling limit ($\Delta_0/k_B T_C = 1.76$), further confirming the strong electron-phonon coupling

TABLE I. The superconducting parameters for TlBi₂ superconductor.

| Parameters (unit) | Value |
|-----------------------------------|-----------------------|
| T_C (K) | 6.2 |
| $\mu_0 H_{c1}(0)$ (T) | 1.08×10^{-2} |
| $\mu_0 H_{c2}(0)$ (T) | 1.4 |
| ξ_{GL} (nm) | 15.3 |
| λ_{GL} (nm) | 198 |
| κ_{GL} | 12.9 |
| λ_{ep} | 1.38 |
| γ (mJ/mol K ²) | 8.63 |
| $\Delta C_{es}/\gamma T_C$ | 2.32 |
| $\Delta_0/k_B T_C$ | 2.25 |

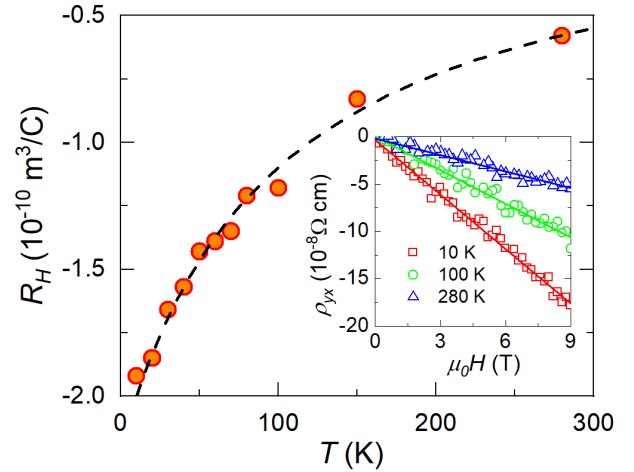


FIG. 4. (Color online) Temperature dependence of the Hall coefficient R_H of TlBi₂ between 10 and 280 K. The dashed line is a guide for eyes. Inset: Isothermal Hall resistivity at $T = 10, 100,$ and 280 K .

in TlBi₂. The obtained superconducting parameters are summarized in Table I.

Figure 4 shows the temperature dependence of the Hall coefficient R_H of TlBi₂. The transverse Hall resistivity, ρ_{yx} , was derived from the antisymmetric part of the transverse resistivity under the reversal of magnetic field at a given temperature. As shown in the inset of Fig. 4, the ρ_{yx} exhibits a linear dependence with the magnetic field below 9 T, suggesting that R_H is independent of the magnetic field. At $T = 10 \text{ K}$, R_H is about $-1.9 \times 10^{10} \text{ m}^3/\text{C}$, indicating that the dominant carriers are electron-type. With increasing temperature, R_H increases monotonically, but remains negative below 300 K. The significant T -dependent behavior of R_H is similar to that observed in MgB₂²². If we assume that the Drude relation holds for TlBi₂ even in the case of multiple bands, the carrier concentration n could be estimated to be $3.3 \times 10^{22}/\text{cm}^3$ at $T = 10 \text{ K}$. Assuming a parabolic dispersion with spherical Fermi surface, the Fermi wave vector, k_F , could be calculated to be $9.9 \times 10^9 \text{ m}^{-1}$ from $k_F = (3n\pi^2)^{1/3}$. Then the band Sommerfeld coeffi-

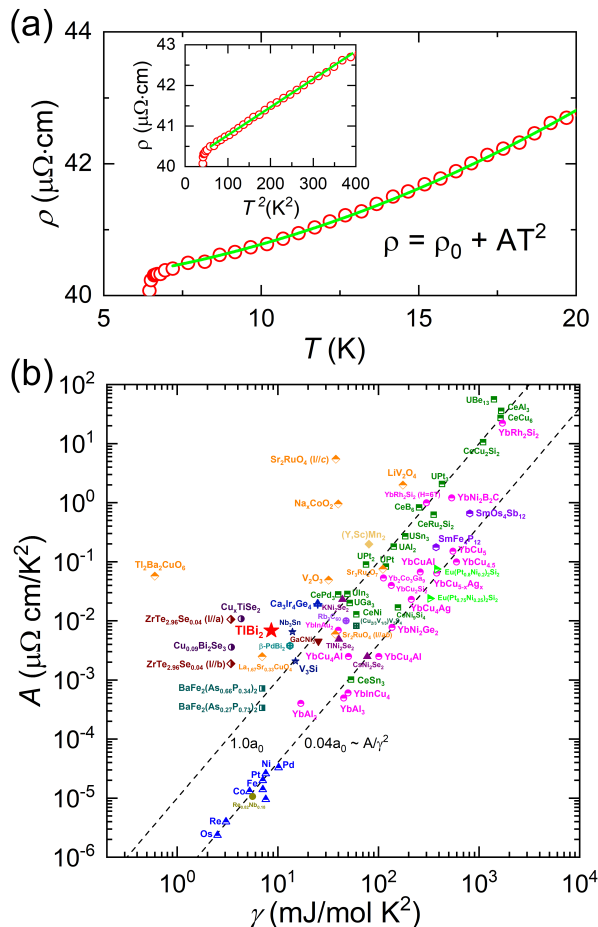


FIG. 5. (Color online) (a) Temperature dependence of resistivity below 20 K; Inset: temperature square dependence of resistivity below 20 K; The solid green lines correspond to $\rho = \rho_0 + AT^2$, just as mentioned in the main text; (b) The coefficient A vs. the Sommerfeld coefficient γ for various compounds. The data beyond TlBi_2 were collected from previous papers²⁴, including CDW materials^{25,26}, oxides^{27–32}, A-15 superconductors³³, heavy fermions^{32,34,35}, transition metals³⁶, and so on^{37,38}.

coefficient γ_b was calculated to be $3.0 \text{ mJ}/(\text{mol K}^2)$ from the relation $\gamma_b = \pi^2 n k_B^2 m_e / \hbar^2 k_F^2$. In a strong coupling compound, the electronic specific heat coefficient γ_{cal} is expected to enhance to be $(1 + \lambda_{ep})\gamma_b$ due to electron-phonon coupling^{16,23}, where λ_{ep} is the electron-phonon coupling constant. Using the value for λ_{ep} (1.38) determined from our measurements, the γ_{cal} is calculated to be $7.14 \text{ mJ}/(\text{mol K}^2)$, which is close to that obtained from the specific heat measurements, indicating that the Fermi-liquid theory can well described the behavior of TlBi_2 compound.

The KWR compares the temperature dependence of a metal's resistivity to that of its specific heat^{34,36}, thereby probing the relationship between the electron-electron scattering rate and the renormalization of the electron mass, which is considered as a measurement of the electron-electron correlation strength. To deduce

the KWR value of TlBi_2 , we fitted the $\rho(T)$ data between 7 and 20 K using the Fermi-liquid prediction, $\rho = \rho_0 + AT^2$, when electron-electron scattering dominates over electron-phonon scattering. The residual resistivity $\rho_0 = 40.1 \mu\Omega \text{ cm}$ and the coefficient $A = 6.84 \times 10^{-3} \mu\Omega \text{ cm}/\text{K}^2$ were obtained by the fitting, as shown in Fig. 5(a). Using the Sommerfeld coefficient $\gamma = 8.63 \text{ mJ}/(\text{mol K}^2)$ obtained from $C(T)$ measurement, we obtained the KWR of TlBi_2 to be $9.2 \times 10^{-5} \mu\Omega \text{ cm}(\text{mol K}^2/\text{mJ})^2$. For many heavy-fermion compounds, the KWR value is close to $1.0 \times 10^{-5} \mu\Omega \text{ cm}(\text{mol K}^2/\text{mJ})^2 = 1.0a_0$, while for a lot of transition metals, the KWR value is close to $0.04 \times 10^{-5} \mu\Omega \text{ cm}(\text{mol K}^2/\text{mJ})^2 = 0.04a_0$ ^{31,34}, where $a_0 = 10^{-5} \mu\Omega \text{ cm}(\text{mol K}^2/\text{mJ})^2$. For a comparison, we plot the KWR for various compounds in Fig. 5(b). It is obvious that the KWR value of TlBi_2 obtained here is somehow unexpectedly larger than that obtained in many heavy Fermi compounds, because the electron correlation seems not so strong as discussed above. It has been argued that the KWR in the heavy fermions is larger than that in transition metals due to the stronger correlation³³. However, several scenarios have been proposed to explain the large KWRs observed in UBe_{13} , transition metals oxides and organic charge-transfer salts, including scattering³³, proximity to a quantum critical point²⁸, as well as the suggestion that electron-phonon scattering in reduced dimensions may result in a quadratic temperature dependence of the resistivity³⁹. Especially, Matsuura *et al.*^{40,41} suggested that the strong dynamical coupling between conduction electrons and phonons may give rise to the heavy fermi bands at low temperatures. Thus, the strong coupling compounds may obey the universal KWR of heavy fermi compounds, *i.e.*, $A/\gamma^2 \approx 10^{-5} \mu\Omega \text{ cm}(\text{mol K}^2/\text{mJ})^2$. Although we can not determine which mechanism can account for the unexpectedly large KWR in TlBi_2 , it is worth noting that our KWR value is almost an order of magnitude larger than that obtained in many heavy Fermi compounds, suggesting that this compound may provide a novel material platform for the study of large KWR.

IV. CONCLUSION

In summary, we systematically investigated the superconducting and normal state properties of TlBi_2 . Type-II superconductivity with $T_C = 6.2 \text{ K}$, the upper critical field $\mu_0 H_{c2} = 1.4 \text{ T}$, and the lower critical field $\mu_0 H_{c1} = 1.08 \times 10^{-2} \text{ T}$ was revealed by the resistivity and magnetization measurements. It was found that the electronic specific heat in the superconducting state can be well described using a single gap model within the BCS framework. The strong electron-phonon coupling occurs in this compound, confirmed by both the large λ_{ep} (1.38) and the large $\Delta_0/k_B T_C$ (2.25) values, indicating that TlBi_2 is a conventional superconductor. In the normal state, the resistivity exhibits T -linear dependence above

50 K, which is ascribed to the low-energy phonon scattering, and T -square dependence below 20 K, suggesting the Fermi-liquid ground state. Combining the specific heat data at normal state, a large KWR [$9.2 \times 10^{-5} \mu\Omega \text{ cm}(\text{mol K}^2/\text{mJ})^2$] was obtained, which is an order of magnitude larger than that obtained in many heavy Fermi compounds, although the electron correlation is not so strong.

ACKNOWLEDGMENTS

This work was supported by the Ministry of Science and Technology of China under Grant No.

2016YFA0300402 and the National Natural Science Foundation of China (NSFC) (Nos. 11974095, 12074335), and the Fundamental Research Funds for the Central Universities.

* hdwang@hznu.edu.cn

† mhfang@zju.edu.cn

- ¹ J. Nagamatsu, N. Nakagawa, T. Muranaka, Y. Zenitani, and J. Akimitsu, *nature* **410**, 63 (2001).
- ² X. Xi, *Reports on Progress in Physics* **71**, 116501 (2008).
- ³ K.-P. Bohnen, R. Heid, and B. Renker, *Phys. Rev. Lett.* **86**, 5771 (2001).
- ⁴ T. Yildirim, O. Gülseren, J. W. Lynn, C. M. Brown, T. J. Udovic, Q. Huang, N. Rogado, K. A. Regan, M. A. Hayward, J. S. Slusky, T. He, M. K. Haas, P. Khalifah, K. Inumaru, and R. J. Cava, *Phys. Rev. Lett.* **87**, 037001 (2001).
- ⁵ J. M. An and W. E. Pickett, *Phys. Rev. Lett.* **86**, 4366 (2001).
- ⁶ J. Kortus, I. I. Mazin, K. D. Belashchenko, V. P. Antropov, and L. L. Boyer, *Phys. Rev. Lett.* **86**, 4656 (2001).
- ⁷ I. I. Mazin, O. K. Andersen, O. Jepsen, O. V. Dolgov, J. Kortus, A. A. Golubov, A. B. Kuz'menko, and D. van der Marel, *Phys. Rev. Lett.* **89**, 107002 (2002).
- ⁸ H. J. Choi, D. Roundy, H. Sun, M. L. Cohen, and S. G. Louie, *Nature* **418**, 758 (2002).
- ⁹ M. Iavarone, G. Karapetrov, A. E. Koshelev, W. K. Kwok, G. W. Crabtree, D. G. Hinks, W. N. Kang, E.-M. Choi, H. J. Kim, H.-J. Kim, and S. I. Lee, *Phys. Rev. Lett.* **89**, 187002 (2002).
- ¹⁰ K.-H. Jin, H. Huang, J.-W. Mei, Z. Liu, L.-K. Lim, and F. Liu, *npj Computational Materials* **5**, 1 (2019).
- ¹¹ X. Zhou, K. N. Gordon, K.-H. Jin, H. Li, D. Narayan, H. Zhao, H. Zheng, H. Huang, G. Cao, N. D. Zhigadlo, F. Liu, and D. S. Dessau, *Phys. Rev. B* **100**, 184511 (2019).
- ¹² E. Makarkov, *Doklady Akademii Nauk SSSR* **74**, 935 (1950).
- ¹³ R. Dynes, *Solid State Communications* **10**, 615 (1972).
- ¹⁴ T. Claeson and O. Östklint, *Acta Metallurgica* **22**, 759 (1974).
- ¹⁵ Y. Zhou, B. Li, Z. Lou, H. Chen, Q. Chen, B. Xu, C. Wu, J. Du, J. Yang, H. Wang, and M. Fang, *Science China Physics, Mechanics & Astronomy* **64**, 1 (2021).
- ¹⁶ T. Takayama, K. Kuwano, D. Hirai, Y. Katsura, A. Yamamoto, and H. Takagi, *Phys. Rev. Lett.* **108**, 237001 (2012).
- ¹⁷ P. B. Allen and R. C. Dynes, *Phys. Rev. B* **12**, 905 (1975).
- ¹⁸ J. P. Carbotte, *Rev. Mod. Phys.* **62**, 1027 (1990).
- ¹⁹ T. Klimczuk, F. Ronning, V. Sidorov, R. J. Cava, and J. D. Thompson, *Phys. Rev. Lett.* **99**, 257004 (2007).
- ²⁰ B. Mühlischlegel, *Zeitschrift für Physik* **155**, 313 (1959).
- ²¹ P. Vashishta and J. P. Carbotte, *Phys. Rev. B* **10**, 2789 (1974).
- ²² R. Jin, M. Paranthaman, H. Y. Zhai, H. M. Christen, D. K. Christen, and D. Mandrus, *Phys. Rev. B* **64**, 220506(R) (2001).
- ²³ M. Brühwiler, S. M. Kazakov, J. Karpinski, and B. Batlogg, *Phys. Rev. B* **73**, 094518 (2006).
- ²⁴ Y. Fang, W.-L. You, and M. Li, *New Journal of Physics* **22**, 053026 (2020).
- ²⁵ K. E. Wagner, E. Morosan, Y. S. Hor, J. Tao, Y. Zhu, T. Sanders, T. M. McQueen, H. W. Zandbergen, A. J. Williams, D. V. West, and R. J. Cava, *Phys. Rev. B* **78**, 104520 (2008).
- ²⁶ X. Zhu, W. Ning, L. Li, L. Ling, R. Zhang, J. Zhang, K. Wang, Y. Liu, L. Pi, Y. Ma, H. Du, M. Tian, Y. Sun, C. Petrovic, and Y. Zhang, *Scientific Reports* **6**, 1 (2016).
- ²⁷ Y. Maeno, K. Yoshida, H. Hashimoto, S. Nishizaki, S.-i. Ikeda, M. Nohara, T. Fujita, A. P. Mackenzie, N. E. Hussey, J. G. Bednorz, and F. Lichtenberg, *Journal of the Physical Society of Japan* **66**, 1405 (1997).
- ²⁸ S. Y. Li, L. Taillefer, D. G. Hawthorn, M. A. Tanatar, J. Paglione, M. Sutherland, R. W. Hill, C. H. Wang, and X. H. Chen, *Phys. Rev. Lett.* **93**, 056401 (2004).
- ²⁹ C. Urano, M. Nohara, S. Kondo, F. Sakai, H. Takagi, T. Shiraki, and T. Okubo, *Phys. Rev. Lett.* **85**, 1052 (2000).
- ³⁰ S. Nakamae, K. Behnia, N. Mangkorntong, M. Nohara, H. Takagi, S. J. C. Yates, and N. E. Hussey, *Phys. Rev. B* **68**, 100502(R) (2003).
- ³¹ A. Jacko, J. Fjærestad, and B. Powell, *Nature Physics* **5**, 422 (2009).
- ³² N. Tsujii, K. Yoshimura, and K. Kosuge, *Journal of Physics: Condensed Matter* **15**, 1993 (2003).
- ³³ K. Miyake, T. Matsuura, and C. Varma, *Solid state communications* **71**, 1149 (1989).
- ³⁴ K. Kadowaki and S. Woods, *Solid state communications* **58**, 507 (1986).
- ³⁵ N. Tsujii, H. Kontani, and K. Yoshimura, *Phys. Rev. Lett.* **94**, 057201 (2005).
- ³⁶ M. J. Rice, *Phys. Rev. Lett.* **20**, 1439 (1968).

- ³⁷ H. Wang, C. Dong, Q. Mao, R. Khan, X. Zhou, C. Li, B. Chen, J. Yang, Q. Su, and M. Fang, *Phys. Rev. Lett.* **111**, 207001 (2013).
- ³⁸ H. Chen, J. Yang, C. Cao, L. Li, Q. Su, B. Chen, H. Wang, Q. Mao, B. Xu, J. Du, and M. Fang, *Superconductor Science and Technology* **29**, 045008 (2016).
- ³⁹ C. Strack, C. Akinci, V. Paschenko, B. Wolf, E. Uhrig, W. Assmus, M. Lang, J. Schreuer, L. Wiehl, J. A. Schlueter, J. Wosnitzer, D. Schweitzer, J. Müller, and J. Wykhoff, *Phys. Rev. B* **72**, 054511 (2005).
- ⁴⁰ T. Matsuura and K. Miyake, *Journal of the Physical Society of Japan* **55**, 610 (1986).
- ⁴¹ C. C. Yu and P. W. Anderson, *Phys. Rev. B* **29**, 6165 (1984).